Luminescent Surface Quaternized Carbon Dots

Athanasios B. Bourlinos,[†,‡] Radek Zbořil,[‡,*] Jan Petr,[‡] Aristides Bakandritsos,[§] Marta Krysmann,[‖] and Emmanuel P. Giannelis[‖,*]

[†]Physics Department, University of Ioannina, GR-45110 Ioannina, Greece

[‡]Regional Centre of Advanced Technologies and Materials, Faculty of Science, Departments of Physical and Analytical Chemistry, Palacky University in Olomouc, 77146, Czech Republic

[§]Department of Materials Science, University of Patras, 26504 Rio, Patras, Greece

[‖]Materials Science and Engineering, Cornell University, Ithaca, New York 14853, United States

Ⓢ *Supporting Information*

Carbon dots (or C-dots) define a new class of functional nanocarbons that have recently drawn considerable attention thanks to their inherently unique photoluminescent properties.[1−7] In general, three main characteristics distinguish C-dots: (i) they consist of discrete, quasi-spherical nanoparticles with sizes below 10 nm, (ii) they are surface-passivated by organic ligands, and (iii) they display multicolor emission in the visible region. Several methods have been already demonstrated for the synthesis of C-dots.[6,7] Among them, the synthesis by thermal oxidation of molecular organic salts combining the carbon source and the surface modifier in a single precursor is an attractive route.[6−9] This strategy involves thermal oxidation in open air at mild temperatures and leads directly to surface-passivated C-dots with a variety of modifiers.

In earlier reports we have demonstrated the synthesis and photoluminescence properties of surface modified C-dots by thermal oxidation of ammonium citrate salts based on octadecylamine, diethylene glycol amine, or sodium 11-aminoundecanoate.[8,9] In these examples the citrate served as the source of carbon and the organic ammonium ions as the surface modifier. Herein we present an alternative molecular synthesis of a new type of light-emitting surface quaternized C-dots. The new method comprises thermal oxidation of a novel salt precursor made from the acid−base combination of tris(hydroxymethyl)aminomethane (Tris) and betaine hydrochloride into the corresponding ammonium carboxylate complex (Figure 1). Tris and betaine are low cost reagents widely used in biology/biochemistry studies. In contrast to our earlier work, the carbon source in this system is provided by Tris and the surface modifier by betaine. More importantly, the new precursor leads to highly uniform dots in terms of their size and charge. Betaine is attached on the outer surface of the nanoparticles through amide linkages formed in situ by thermal condensation of the ammonium carboxylate groups (e.g., $-NH_3^+{}^-OOC- \rightarrow -NHCO- + H_2O$).[8,9] In addition, the ionic character of the betaine ligand confers the functionalized nanoparticles dispersibility in water and anion-exchange capacity. The nanoparticles fluoresce in the visible region with long-term fluorescence/colloidal stability in water even after exposure to high temperature/high pressure conditions.
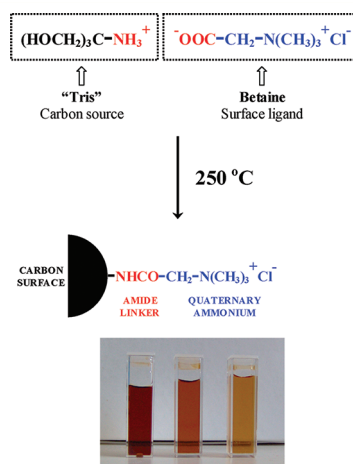

Figure 1. Synthesis and structure of the water-dispersible QC-dots. The photo at the bottom shows aqueous dispersions with concentrations of 2, 1, and 0.5 mg mL^{-1}, respectively (left to right).

The dots were further characterized by capillary electrophoresis confirming homogeneous and stable colloidal dispersions of cationic nanoparticles with highly uniform size and surface charge density. These features together with the unique structural uniformity of the dots make the present approach more advantageous over the citrate method.

The surface quaternized C-dots (abbreviated thereafter QC-dots) were prepared as follows: 1.5 g betaine hydrochloride (Alfa Aesar) was dissolved in 5 mL of water resulting in a strongly acidic solution. Subsequently, 1.2 g Tris (Aldrich) was added to the betaine hydrochloride solution until complete dissolution (1:1 molar ratio). The pH of the initially acidic solution became neutral after addition of the Tris base. The water-soluble organic salt was partly recovered from the solution using an excess of isopropanol (100 mL). The obtained syrup was then rinsed and washed three times with

100 mL of isopropanol. The whole process was repeated two additional times in order to collect enough precursor material (ca. 1−2 mL). The combined portions were dried for 1−3 days at 80 °C using infrequent stirring with a spatula. The resulting viscous white mass was directly heated at 250 °C in air for 2 h in a porcelain crucible (35 cm^3 capacity). This temperature is adequate for the carbonization of Tris while simultaneously protecting betaine from degradation. Thermal treatment led to volume expansion resulting in a brown solid. A large part of the solid was discarded as nondispersible and the fractions near the walls and the bottom of the crucible were extracted with 25 mL of water. The deep brown aqueous dispersion formed was passed through a large pore filter paper in order to remove any insoluble particulates. QC-dots were precipitated from the colloid by adding 200 mL of acetone. The precipitate was left to settle down, and the supernatant liquid was discarded. QC-dots were rinsed and washed three times with 200 mL of acetone and air-dried at ambient conditions to afford a dark brown powder. Elemental Analysis (w/w %): C, 55.15; H, 6.79; N, 11.05; O, 19.51; Cl, 7.50. The chloride content corresponds to an anion-exchange capacity of 2.1 mmol g^{-1}.

Because of the quaternary ammonium chloride present, QC-dots are highly dispersible in water (>20 mg mL^{-1}) and produce stable colloids with a zeta potential of +43 mV and relatively narrow, symmetric distribution (Supporting Information Figure S1). The positively charged dots flocculate with bulky anions (e.g., ferrocyanides, iodides) or at high chloride concentrations (e.g., brine) while readily interacting with substrates bearing negative charge (clays, zeolites, biomolecules, or dyes). Transmission electron microscopy (TEM) reveals the formation of nearly spherical nanoparticles with sizes in the range 4−9 nm (Figure 2). The TEM results agree well with the
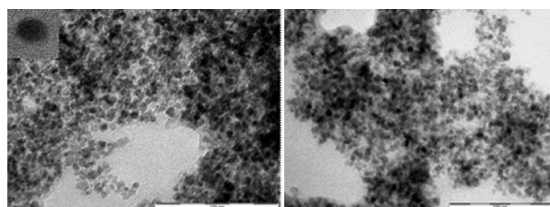

Figure 2. TEM images of QC-dots (the top inset displays a single nanoparticle). The scale bar is 100 nm.

average particle size of 7 nm obtained from dynamic light scattering (DLS) in water (Supporting Information Figure S2).

The QC-dots are amorphous based on powder X-ray diffraction. Thermal gravimetric analysis in air (TGA) shows a weight loss (T < 100 °C) attributed to water loss from the hydrated ionic nanoparticles (15%), a second step (T > 280 °C) due to the decomposition of the betaine ligand (27%), and a third double step (T > 400 °C) attributed to the combustion of the carbon-based core containing both aliphatic and aromatic domains (58%) (Supporting Information Figure S3). The aliphatic part usually contains a large fraction of H and O atoms, which are removed thermally before combustion of the polyaromatics. Assuming that the betaine segment on the surface of the QC-dots corresponds to —(O=)CCH$_2$N-(CH$_3$)$_3$$^+Cl^-$, then the weight loss of 27% provides an anion-exchange capacity of ca. 2 mmol g^{-1}, in excellent agreement with the 2.1 mmol g^{-1} estimated from the chloride elemental analysis (vide supra). Infrared spectroscopy (IR) shows characteristic bands between 2850 and 3000 cm^{-1} and 1350−

1470 cm^{-1} for the CH$_2$ and CH$_3$ groups of the betaine ligand, two absorption peaks at 1650 cm^{-1} and 1575 cm^{-1} assigned to the amide I and amide II bands of the —NHCO— linker, several absorptions between 950 and 1200 cm^{-1} due to C—O vibrations within the oxygen-containing core, and a broad band at 600 cm^{-1} typically present in many carbonaceous solids and ascribed to graphitic domains (Supporting Information Figure S4). Proton nuclear magnetic resonance (^{1}H NMR) analysis in D$_2$O shows two single peaks due to betaine: one at 1.1 ppm for the methyl groups in N(CH$_3$)$_3$ and another at 2.6 ppm for the methylene group in NCH$_2$ (Supporting Information Figure S5). These two peaks correspond well to the proton ratio of methyl/methylene groups in betaine. Besides these two signals, an additional single peak at 2.1 ppm attributed to methylene groups close to phenyl rings (ArCH$_2$) can also be seen. This peak probably originates from the aliphatic part of the carbon-based core, which coexists with aromatic domains. Residual methylene groups are expected to be present in the core from the Tris carbon source after a mild thermal treatment.

The absorption−emission spectra of QC-dots are shown in Figure 3 (excitation−emission spectra are given in Supporting
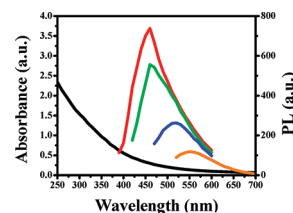

Figure 3. Absorption (black line) and wavelength-dependent emission (colored lines) spectra of QC-dots in water. Emission for excitations at 375 and 400 nm occurs at 460 nm (red and green), whereas emission for excitations at 450 and 500 nm occurs at 520 (dark blue) and 550 nm (orange), respectively.

Information Figure S6). The absorption spectrum in water revealed no distinct peaks in the UV−vis region. With respect to the fluorescence spectra, when the excitation wavelength was between 375 and 400 nm the emission wavelength remained stable, indicating that one fluorescent species dominates the emission of the dots in this UV region.[10,11] When the excitation wavelength varied from 400 to 500 nm, the fluorescence spectra red-shifted and the intensity decreased gradually. This fluorescence behavior suggests the presence of different types of fluorophores having different degrees of double bond conjugation and, hence, different emission wavelengths.[10,11] The quantum yield was calculated at 4%, relative to anthracene ethanol solution in line with other C-dots.[12] The PL intensity of aqueous dispersions of QC-dots was investigated for samples heated at 100 °C for the periods of 72, 96, and 144 h (Figure 4). To this end, aqueous dispersions were sealed in glass vials (filled to 90% capacity) and heated at 100 °C for varying periods of time under hydrothermal conditions.[13] The PL for all samples was measured at room temperature using different excitation wavelengths. For comparison, the PL of the sample that was not heated at 100 °C is also included (t = 0 h). It was observed that the fluorescence intensity initially increased[13] and then remained stable, indicating long-term fluorescence stability. In addition, no precipitation was observed, suggesting long-term colloidal stability as well.

To investigate the uniformity in size and surface chemistry of QC-dots we used capillary electrophoresis (CE) as a very
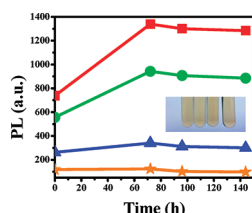
Figure 4. PL intensity of aqueous dispersion of QC-dots as a function of exposure time to high temperature/high pressure conditions, using different excitation wavelengths (excitations at 375 nm, red line; excitations at 400 nm, green line; excitations at 450 nm, dark blue line; excitations at 500 nm, orange line). Inset shows the set of aqueous dispersions used in the experiments with no signs of precipitation.

sensitive analytical technique for the characterization of nanoparticles in different electrolytes.[14−16] CE was used here to compare the behavior of QC-dots with the previously synthesized C-dots based on the citrate method.[8,9] The behavior of these two types of C-dots was tested in two different electrolytes differing in ionic strength and hydrophobicity: (i) 35 mM sodium acetate, pH 4.5, and (ii) 35 mM sodium borate pH 9.5 with 150 mM SDS (sodium dodecyl sulfate). As a general trend, QC-dots showed more symmetrical and narrower peaks in comparison to the citrate based C-dots, suggesting a more uniform size/charge density for the former. The cationic nature of QC-dots is clearly seen in sodium acetate electrolyte in Figure 5, where cations migrate before
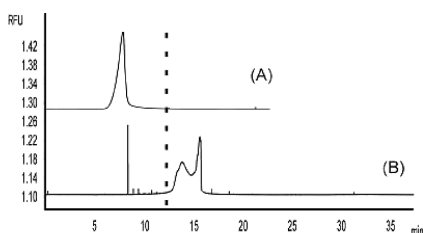

Figure 5. CE characterization of QC-dots (A) and citrate-derived C-dots (B) in acetate electrolyte. Conditions: 35 mM sodium acetate electrolyte pH 4.5, +20 kV, 25 °C; peaks corresponding to the C-dots are in 6.5−8.5 min for (A) and 12.5−16 min for (B); dashed line represents time of migration of a neutral marker.

neutral compounds (dashed line) and the citrate based C-dots migrate as anions (after neutrals). The narrow and single peak suggests a uniform size and charge density for the QC-dots. In contrast, the citrate-derived C-dots exhibit a double peak probably due to size distribution and/or surface charge inhomogeneity of the latter. Pronounced differences between these two types of C-dots were found in the sodium borate electrolyte with SDS (Supporting Information Figure S7). This electrolyte favors hydrophobic interactions, and therefore CE could identify particles with different surface (hydrophobic/hydrophilic) properties. QC-dots showed again a narrow peak while the citrate derived C-dots migrated as a large hump reflecting the structural inhomogeneity of their surfaces. These results clearly confirm that QC-dots exhibit much more uniform size/charge characteristics compared to the citrate derived ones.

In summary, we have presented an alternative molecular synthesis toward a new type of surface quaternized C-dots that are water-dispersible, possess anion-exchange properties, and fluoresce in a continuous manner with long-term stability even

after exposure to high temperature/high pressure conditions. CE experiments confirm the presence of positively charged nanoparticles with highly uniform size/charge. Thanks to these features, the functional dots may show promise for a broad range of applications in place of conventional organic or inorganic light emitters. The method is complementary to the citrate approach and could lead to a library of surface engineered C-dots.

■ ASSOCIATED CONTENT

ⓢ Supporting Information

Zeta potential distribution, DLS particle size distribution, TGA trace, IR/^{1}H NMR spectra, excitation−emission spectra, comparative CE traces in the sodium borate electrolyte with SDS, and materials and methods for CE characterization (PDF). This material is available free of charge via the Internet at http://pubs.acs.org.

■ AUTHOR INFORMATION

Corresponding Author
*E-mail: radek.zboril@upol.cz (R.Z); epg2@cornell.edu (E.P.G.).

■ ACKNOWLEDGMENTS

■ REFERENCES

(1) Sun, Y.-P.; Zhou, B.; Lin, Y.; Wang, W.; Fernando, K. A. S.; Pathak, P.; Meziani, M. J.; Harruff, B. A.; Wang, X.; Wang, H.; Luo, P. G.; Yang, H.; Kose, M. E.; Chen, B.; Veca, L. M.; Xie, S.-Y. *J. Am. Chem. Soc.* **2006**, *128*, 7756.
(2) Liu, H.; Ye, T.; Mao, C. *Angew. Chem., Int. Ed.* **2007**, *46*, 6473.
(3) Mochalin, V. N.; Gogotsi, Y. *J. Am. Chem. Soc.* **2009**, *131*, 4594.
(4) Peng, H.; Travas-Sejdic, J. *Chem. Mater.* **2009**, *21*, 5563.
(5) Zhang, J.; Shen, W.; Pan, D.; Zhang, Z.; Fang, Y.; Wu, M. *New J. Chem.* **2010**, *34*, 591.
(6) Baker, S. N.; Baker, G. A. *Angew. Chem., Int. Ed.* **2010**, *49*, 6726.
(7) Da Silva, J. C. G. E.; Gonçalves, H. M. R. *Trends Anal. Chem.* **2011**, *30*, 1327.
(8) Bourlinos, A. B.; Stassinopoulos, A.; Anglos, D.; Zbořil, R.; Georgakilas, V.; Giannelis, E. P. *Chem. Mater.* **2008**, *20*, 4539.
(9) Bourlinos, A. B.; Stassinopoulos, A.; Anglos, D.; Zbořil, R.; Karakassides, M. A.; Giannelis, E. P. *Small* **2008**, *4*, 455.
(10) Mao, X.-J.; Zheng, H.-Z.; Long, Y.-J.; Du, J.; Hao, J.-Y.; Wang, L.-L.; Zhou, D.-B. *Spectrochim. Acta, Part A* **2010**, *75*, 553.
(11) Sun, W.; Du, Y.; Wang, Y. *J. Lumin.* **2010**, *130*, 1463.
(12) Eaton, D. F. *Pure Appl. Chem.* **1988**, *60*, 1107.
(13) Tian, L.; Song, Y.; Chang, X.; Chen, S. *Scr. Mater.* **2010**, *62*, 883.
(14) Radko, S. P.; Chrambach, A. *Electrophoresis* **2002**, *23*, 1957.
(15) Lopez-Lorente, A. I.; Simonet, B. M.; Valcarcel, M. *Trends Anal. Chem.* **2011**, *30*, 58.
(16) Carrillo-Carrión, C.; Moliner-Martínez, Y.; Simonet, B. M.; Valcárcel, M. *Anal. Chem.* **2011**, *83*, 2807.